

The classical skeleton of open quantum chaotic maps

Lisandro A. Raviola^{1,2}, Alejandro M.F. Rivas², and Gabriel G. Carlo^{2*}

¹*Instituto Sábato (UNSAM - CNEA), Av. Gral. Paz 1499,
B1650KNA San Martín, Buenos Aires, Argentina and*

²*Departamento de Física, CNEA, Av. del Libertador 8250, C1429BNP Buenos Aires, Argentina*
(Dated: December 25, 2021)

Abstract

We have studied two complementary decoherence measures purity and fidelity for a generic diffusive noise in two different chaotic systems (the baker and the cat maps). For both quantities, we have found classical structures in quantum mechanics – the scar functions – that are specially stable when subjected to environmental perturbations. We show that these quantum states constructed on classical invariants are the most robust significant quantum distributions in generic dissipative maps.

PACS numbers: 05.45.Mt, 03.65.Sq, 03.65.Yz

I. INTRODUCTION

In quantum chaos (i.e. the study of quantum systems whose classical counterparts are chaotic), the complete description of the eigenfunctions is still an open problem. While there is a semiclassical method for obtaining the eigenstates of an integrable system (the well-known EBK/WKB quantization scheme [1, 2]), the same problem in the chaotic case has proven harder to solve. One of the major advances in this sense has been Gutzwiller's theory of periodic orbits for the quantum chaotic spectra [3], devised in the early 70's.

A recently developed approach allows to obtain all the information of a generic quantum system by just using the shortest periodic orbits of its classical counterpart [4]. This formalism has been successfully applied to the description of the eigenstates of many chaotic quantum systems like for example, the Bunimovich's billiard [5], the cat map [6] and the baker map [7]. These results suggest that states built using only this classical information (the so-called *scar functions*) constitute the skeleton of the eigenstates of any quantum chaotic system.

On the other hand, taking into account the restoration of the classical dynamics induced by decoherence in an open quantum system [8] and the behavior of distributions against external perturbations [9–11] we can ask ourselves: are scar functions, as a consequence of their classical content, more robust than other states facing an environment-induced decoherence? Trying to answer this question, in [12] we have studied a very simple model of a chaotic quantum system interacting with an environment that produces dissipation and decoherence (an *open quantum map*). In this article, we exhaustively expand the results presented there by studying different open maps. This leads us to our main result, i.e. we show here that scar functions are the most robust significant quantum distributions in generic dissipative maps.

In this paper we study the behavior of classically moti-

vated states (by analyzing two different measures, namely the purity and fidelity) corresponding to two paradigmatic systems in quantum chaos, the baker map and the cat map on the torus [13, 14]. We introduce decoherence by means of a diffusive noise model [15]. We have organized this work as follows. In section 2, we describe the main theoretical tools we need throughout our investigations (open quantum maps and scar functions). In Section 3 we define the maps considered. Section 4 presents our results. In section 5 we come to some conclusions.

II. THEORETICAL TOOLS

Open quantum maps are the simplest systems that capture all the essential features of chaotic dynamics and dissipation. As such, they are the ideal testbed for studying the effect of the environment on quantum distributions. Our main interest is focused on determining how the classical information emerges from the quantum structures. For that purpose we will make use of the scar functions, whose construction we explain at the end of this Section.

A. Open quantum maps

The quantization of maps on a compact phase space proceeds in two stages: a kinematic one, which establishes the Hilbert space appropriate to the phase space geometry, and a dynamical one, which consists in defining a suitable quantum operator corresponding to the classical dynamics. Finally, Kraus operators take into account the effect of the environment.

1. Kinematics

In this work, the classical phase space associated with the systems under investigation is the 2-dimensional torus $\mathbb{T}^2 = \mathbb{R}^2/\mathbb{Z}^2$, consisting of a square of unit side with opposite sides identified. Points in this space have

*Electronic address: raviola@tandar.cnea.gov.ar

coordinates $(q, p) \in [0, 1) \times [0, 1)$. To be compatible with the phase space geometry, quantum wave functions must be periodic in both position and momentum (up to a phase)

$$\psi(q+1) = \exp(-i2\pi\chi_q) \psi(q) \quad (1)$$

$$\tilde{\psi}(p+1) = \exp(i2\pi\chi_p) \tilde{\psi}(p) \quad (2)$$

with

$$\tilde{\psi}(p) = \frac{1}{\sqrt{2\pi\hbar}} \int_{-\infty}^{\infty} dq e^{-\frac{i}{\hbar}qp} \psi(q). \quad (3)$$

The phases $2\pi\chi_q, 2\pi\chi_p$ are called *Floquet's angles*, with $0 \leq \chi_q, \chi_p < 1$. Periodicity in q and p implies

$$2\pi\hbar N = 1 \quad (4)$$

This means that the Hilbert space of wave functions \mathcal{H}_N , the quantum counterpart of the classical compact phase space, is effectively finite-dimensional with dimension N . In this context, the semi-classical limit $\hbar \rightarrow 0$ is equivalent to taking $N \rightarrow \infty$.

The usual canonical commutation relations between position and momentum operators (which are the generators of *infinitesimal* translations in phase space) do not hold in the finite-dimensional case, so we can't define position and momentum operators \hat{q}, \hat{p} . However, we can define *finite* displacement operators \hat{U} and \hat{V} , whose form is analogous to that of the infinite-dimensional case. These operators are unitary and its eigenvectors form a basis for \mathcal{H}_N [16–19].

The basis of position vectors $|q_j\rangle$ for this space will be defined from the eigenvectors of the momentum displacement operator \hat{V}

$$\hat{V}|q_j\rangle = \exp\left[\frac{2\pi i}{N}(j + \chi_q)\right] |q_j\rangle, \quad j \in [0, N-1] \quad (5)$$

The position in phase space associated with $|q_j\rangle$ is

$$q_j = \frac{j + \chi_q}{N}. \quad (6)$$

Analogously, the momentum vectors $|p_k\rangle$ satisfy

$$\hat{U}|p_k\rangle = \exp\left[-\frac{2\pi i}{N}(k + \chi_p)\right] |p_k\rangle \quad (7)$$

$$p_k = \frac{k + \chi_p}{N}, \quad k \in [0, N-1] \quad (8)$$

where \hat{U} is the position displacement operator.

These bases are related by means of a discrete Fourier transform

$$\langle p_k | q_j \rangle = N^{-\frac{1}{2}} \exp\left[-\frac{2\pi i}{N}(j + \chi_q)(k + \chi_p)\right] \equiv \hat{F}_N^{j,k} \quad (9)$$

From the previous equations, it can be shown that [16–19]

$$\hat{U}|q_j\rangle = |q_{j+1}\rangle \quad (10)$$

$$\hat{U}^N|q_j\rangle = |q_{j+N}\rangle = \exp(-i2\pi\chi_q) |q_j\rangle \quad (11)$$

$$\hat{V}|p_k\rangle = |p_{k+1}\rangle \quad (12)$$

$$\hat{V}^N|p_k\rangle = |p_{k+N}\rangle = \exp(i2\pi\chi_p) |p_k\rangle \quad (13)$$

These operators satisfy the relation

$$\hat{U}^j \hat{V}^k = \hat{V}^k \hat{U}^j \exp\left(\frac{2\pi i}{N}jk\right) \quad (14)$$

With them, we can define a discrete version of the phase space displacement operator

$$\hat{T}_{j,k} = \frac{1}{\sqrt{N}} \exp\left(\frac{i\pi}{N}jk\right) \hat{V}^j \hat{U}^k \quad (15)$$

with the property $\hat{T}_{j,k}^\dagger = \hat{T}_{-j,-k}$. The set $\left\{\hat{T}_{j,k}\right\}_{j,k=0}^{N^2-1}$ of finite displacements forms a basis for the Hilbert space $\mathcal{H}_{N^2} = \mathcal{H}_N \otimes \mathcal{H}_N^*$ of linear operators on \mathcal{H}_N (Liouville space) with the Hilbert-Schmidt inner product

$$(\hat{A}, \hat{B}) = \text{Tr}\left(\hat{A}^\dagger \hat{B}\right) \quad (16)$$

This basis of N^2 displacement operators satisfies

$$\text{Tr}\left(\hat{T}_{j,k}^\dagger \hat{T}_{j',k'}\right) = \delta_{j,j'} \delta_{k,k'} \quad (17)$$

so it constitutes a complete orthonormal set.

2. Dynamics

By virtue of the finite dimension of \mathcal{H}_N , the quantum dynamics is given by a unitary $N \times N$ matrix \hat{U}_N and the system state evolution is obtained by means of a straightforward matrix multiplication. In our case, this matrix will be the quantization of a classical (chaotic) map P on \mathbb{T}^2 . This means that, given the mapping $P(q, p)$, there exists a sequence of unitary operators \hat{U}_N (called *quantum map*) acting on \mathcal{H}_N such that the so-called Egorov property is fulfilled, i.e.

$$\lim_{N \rightarrow \infty} \left\| \hat{U}_N^{-1} \text{Op}(f) \hat{U}_N - \text{Op}(f \circ P) \right\| = 0 \quad \forall f \in C^\infty(\mathbb{T}^2) \quad (18)$$

$\text{Op}(f)$ represents the Weyl quantization of the observable f [16].

3. Environment

If the quantum system interacts with an environment, the elements (kets) of \mathcal{H}_N no longer represent its state. In this situation, all that can be said about the system at

time t is encoded in its associated density operator $\hat{\rho}_t$ [20–22]. The evolution of $\hat{\rho}_t$ is given, under sufficiently general conditions, by a completely positive, trace-preserving map \mathbf{S} of density matrices into density matrices called *superoperator* or *quantum operation* [21–23].

In this context, we define an *open quantum map* \mathbf{S} [15, 24] as a map whose action can be written in the form of a product of two superoperators

$$\hat{\rho}_{t+1} = \mathbf{S}(\hat{\rho}_t) = \mathbf{D}_\varepsilon \mathbf{M}(\hat{\rho}_t) \quad (19)$$

$\mathbf{M}(\hat{\rho}_t) = \hat{M}\hat{\rho}_t\hat{M}^\dagger$ is a map that generates the unitary evolution of the system, \hat{M} being the evolution operator that acts upon elements of the Hilbert space associated to the non-interacting system. \mathbf{D}_ε is a superoperator that models the interaction between system and environment according to a set of parameters ε related to the specific type of interaction. This last superoperator is responsible for introducing noise in the –otherwise unitary– system evolution.

In the present work, \hat{M} will be the quantization of a classically chaotic map acting on the torus. In particular, we will consider two completely chaotic maps: the baker map and the cat map [13, 14]. Besides, the noise superoperator will be expressed according to the Kraus representation [21–23], which in general can be expressed as

$$\mathbf{D}_\varepsilon(\hat{\rho}_t) = \sum_{i=0}^{N^2-1} \hat{K}_i \hat{\rho}_t \hat{K}_i^\dagger \quad (20)$$

with $\sum_i \hat{K}_i^\dagger \hat{K}_i = \mathbb{1}$ in order to preserve the trace of $\hat{\rho}_t$. The way the system interacts with the environment will be completely determined by the Kraus operators \hat{K}_i . In the following Section, we will define these operators explicitly. An example of the action of the environment in phase space can be seen in Figs. 1 and 2.

B. Scar functions

The semiclassical theory of short periodic orbits [4] is a formalism that allows to obtain all the quantum information of a chaotic Hamiltonian system in terms of a very small number of short periodic orbits. The main elements in this theory are the so-called *scar functions*. These are wavefunctions highly localized in the neighborhood of the classical periodic orbits and on their stable and unstable manifolds, satisfying a Bohr-Sommerfeld quantization condition along the trajectory. They are defined for Hamiltonian flows as

$$|\phi_{scar}\rangle = \int_{-T}^T dt \cos\left(\frac{\pi t}{2T}\right) e^{\frac{i}{\hbar}(E_{BS}-\hat{H})t} |\phi_{tube}\rangle \quad (21)$$

where \hat{H} is the system’s Hamiltonian, T is of the order of Ehrenfest’s time, and $|\phi_{tube}\rangle$ is a wavefunction localized on the periodic orbit with Bohr-quantized energy E_{BS} .

In [6, 7] the formalism has been adapted to quantum maps on the torus, and the resulting formula for scar functions is given in terms of a sum

$$|\phi_{scar}^{maps}\rangle = \sum_{t=-T}^T \cos\left(\frac{\pi t}{2T}\right) e^{\frac{i}{\hbar}E_{BS}t} \hat{U}^t |\phi_{POM}^{maps}\rangle \quad (22)$$

where \hat{U} is the evolution operator of the quantum map and $|\phi_{POM}^{maps}\rangle$ (called *Periodic Orbit Mode* or POM) is a sum of coherent states on the torus centered at the fixed points of a given periodic orbit, each one having a phase. In this case, the Ehrenfest time is $T = \frac{\ln N}{\lambda}$, λ is the Lyapunov exponent of the map and N is the Hilbert space dimension.

As an example, the upper right panels of Figs. 3 and 4 show Husimi representations of scar functions constructed for the baker map and for the cat map, respectively. It’s clearly visible the enhancement of probability that these wavefunctions have on the corresponding periodic orbit and its stable and unstable manifolds.

III. SYSTEMS

A. Baker map

The first model of chaotic dynamics we consider is the baker map $B : \mathbb{T}^2 \rightarrow \mathbb{T}^2$, given by the transformation [13, 14]

$$(q', p') = B(q, p) = [2q - [2q], (p + [2q])/2] \quad (23)$$

where $[x]$ stands for the integer part of x . This transformation is an area-preserving, uniformly hyperbolic, piecewise-linear and invertible map with Lyapunov exponent $\lambda = \ln 2$. The vertical (horizontal) lines $q = q_0$ ($p = p_0$) represent the stable (unstable) manifolds.

The phase space has a very simple Markov partition consisting of two regions ($q < 1/2$ and $q \geq 1/2$) associated with the symbols 0 and 1, for which there is a complete symbolic dynamics. The action of the map upon symbols can be understood by means of the binary expansion of the coordinates

$$(p|q) = \dots \nu_{-1} \cdot \nu_0 \nu_1 \dots \xrightarrow{B} (p'|q') = \dots \nu_{-1} \nu_0 \cdot \nu_1 \dots \quad (24)$$

where $q = \sum_{i=0}^{\infty} \nu_i 2^{-(i+1)}$ and $p = \sum_{i=-1}^{-\infty} \nu_i 2^i$. Then, a periodic orbit of period L can be represented by a binary string $\boldsymbol{\nu}$ of length L . The coordinates of the first trajectory point (q_0, p_0) on the periodic orbit can be obtained explicitly in terms of the binary string as $q_0 = \cdot \boldsymbol{\nu} \boldsymbol{\nu} \dots = \nu/(2^L - 1)$ and $p_0 = \cdot \boldsymbol{\nu}^\dagger \boldsymbol{\nu}^\dagger \boldsymbol{\nu}^\dagger \dots = \nu^\dagger/(2^L - 1)$, where ν is the integer value of the string $\boldsymbol{\nu}$ which represents a binary number, and $\boldsymbol{\nu}^\dagger$ is the string formed by all L bits of $\boldsymbol{\nu}$ in reverse order. The other trajectory points can be easily calculated by iterations of the map or by cyclic shifts of $\boldsymbol{\nu}$.

The unitary operator \hat{M} that performs the closed quantum evolution is given in position representation by [25, 26]

$$\hat{M} = \hat{F}_N^\dagger \begin{pmatrix} \hat{F}_{N/2} & \mathbb{O} \\ \mathbb{O} & \hat{F}_{N/2} \end{pmatrix} \quad (25)$$

where \hat{F}_N is the N -dimensional Fourier transform operator whose matrix elements were defined in (3). Throughout the paper we assume for the quantum baker map a phase space with anti-symmetric boundary conditions ($\chi_q = \chi_p = 1/2$) in order to preserve the classical map symmetries [26].

B. Cat map

Another simple model with strongly chaotic dynamics on \mathbb{T}^2 is the cat map [13, 14]. It's an invertible, area-preserving canonical transformation A whose matrix has integer entries, and with $\text{Tr}(A) > 2$ to ensure hyperbolicity. A common choice for A is

$$\begin{pmatrix} q' \\ p' \end{pmatrix} = A \begin{pmatrix} q \\ p \end{pmatrix} = \begin{pmatrix} 2 & 1 \\ 3 & 2 \end{pmatrix} \begin{pmatrix} q \\ p \end{pmatrix} \pmod{1} \quad (26)$$

The Lyapunov exponent for this map is $\lambda = \ln(2 + \sqrt{3}) \approx 1.317$. The expanding and contracting eigenspaces through the origin are given by $\xi_u = (-\sqrt{3}, 1)$ and $\xi_s = (\sqrt{3}, 1)$. The irrational slope of the two directions implies that stable and unstable linear manifolds are densely distributed over the torus.

The map is quantized by means of its generating function [14, 27], giving a unitary propagator \hat{M} whose matrix elements in position representation are

$$\hat{M}_{j,k} = \frac{1}{\sqrt{N}} \exp \left[\frac{2\pi i}{N} (j^2 - jk + k^2) \right] \quad (27)$$

C. Noise model

We define the superoperator D_ε by means of translation operators on the torus [15]

$$D_\varepsilon(\hat{\rho}_t) = \sum_{j,k=0}^{N-1} c_\varepsilon(j,k) \hat{T}_{j,k} \hat{\rho}_t \hat{T}_{j,k}^\dagger \quad (28)$$

. These translation operators (our Kraus operators) are defined by Eq. (15). To preserve $\text{Tr}(\hat{\rho}_t)$ we assume $\sum_{j,k=0}^{N-1} c_\varepsilon(j,k) = 1$. This way, the coefficient $c_\varepsilon(j,k)$ represents the probability of a translation being applied on the system in the direction (j,k) . Defining this function as a periodized Gaussian (to satisfy the boundary conditions on the torus)

$$c_\varepsilon(j,k) \propto \sum_{\mu,\nu=-\infty}^{\infty} \exp \left[-\frac{(j - \mu N)^2 + (k - \nu N)^2}{2 \left(\frac{\varepsilon N}{2\pi}\right)^2} \right] \quad (29)$$

we obtain a noise superoperator which has the effect of diffusing the state on a region of radius $\approx \varepsilon$ in phase space. The consequence of this incoherent superposition of translations is decoherence, which can be visualized as the suppression of the small scale interference fringes in the Wigner representation. After a short time, the Wigner function becomes positive and the state appears “smeared out” in phase space. As previously mentioned, this behavior can be seen in Figs. 1 and 2, which show the effect of noise over the discrete Wigner function [16, 17, 19] of a superposition of coherent states. The parameter ε can be interpreted as a measure of the coupling between the system and the environment.

IV. RESULTS

In order to quantify the stability of the states of interest against decoherence, we have calculated the purity

$$P(t) = \text{Tr}(\rho_t^2) \quad (30)$$

and the fidelity or autocorrelation function

$$F(t) = \sqrt{\langle \psi | \rho_t | \psi \rangle} \quad (31)$$

as functions of time. In (31), $|\psi\rangle$ represents the pure initial state, hence $\rho_0 = |\psi\rangle\langle\psi|$.

Purity is a measure of the correlation degree between the system and the environment, and its evolution in time indicates how fast the system loses coherence. Fidelity can be interpreted as the distance between the evolved state and the initial state. Its development in time allows us to measure the velocity with which the evolved state “moves away” from the initial one under the action of the noisy dynamics. Complementarily, this difference between the initial and evolved states can be observed in terms of a density operator representation in phase space, like Husimi or Wigner distribution functions [16, 28].

We have studied the evolution of these quantities from initial states defined as scar functions, periodic orbit modes and eigenstates of the unitary quantum map. For each system, we have built the scar functions and the periodic orbit modes on different short periodic orbits of the corresponding classical map (without noise) and then compared their evolution to those of the map eigenstates, in particular with those localized on or nearer the same orbits. We have also studied the effect of varying the coupling with the environment by means of taking different values for the parameter ε .

In the following Figures, we show some typical results of our numerical calculations. They are illustrative of an exhaustive exploration of the eigenstates of our systems. Fig. 3 shows the behavior of purity and fidelity for the

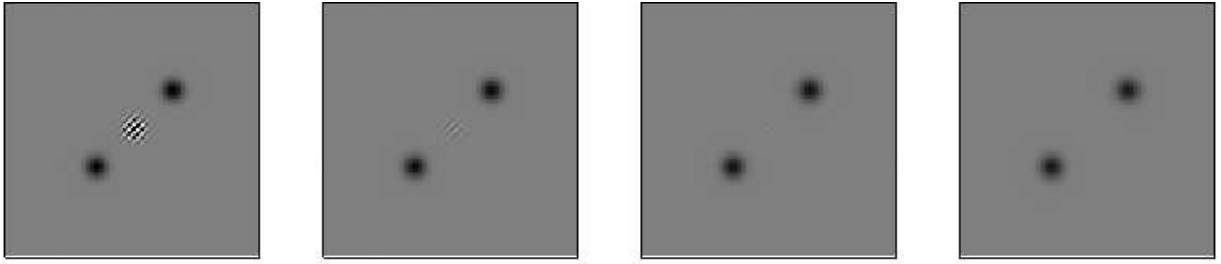


Figure 1: Action of the noise model in phase space. The first panel (left) shows the discrete Wigner function of a superposition of two coherent states centered at $(0.35, 0.35)$ and $(0.65, 0.65)$. The value of the Wigner function is shown using a gray scale from white (minimum, negative) to black (maximum, positive) (same scale for all panels). As time goes on (from left to right) the noise superoperator D_ε acting on the state washes out the interference fringes. We have taken $\varepsilon = 0.05$ and $N = 100$.

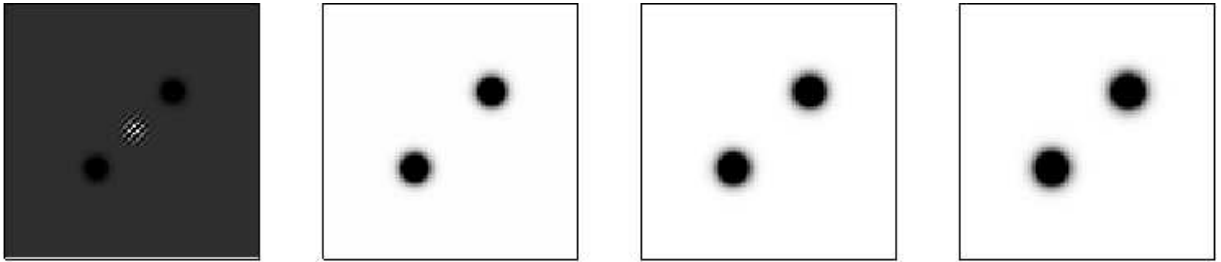


Figure 2: Action of the noise superoperator on the same initial state as in Fig. 1, but with stronger coupling ($\varepsilon = 0.1$). In this case the interference fringes disappear already in the first application of the noise superoperator. The gray scale chosen in this case enhances the visualization of the Wigner function spreading in phase space.

case of the noisy baker map model. The states are localized over a period 2 orbit with symbolic code 01, as can be seen in the Husimi representations of the upper panel. The overlap between the scar function and the map eigenstate is 0.828, so the states are quite similar in terms of this distance measure. However, there is a visibly different behavior in terms of purity and fidelity, favoring the semiclassically constructed states in general, and the scar functions in particular, which lose purity and fidelity at a slower pace.

For the noisy cat map we have a similar behavior, but the differences between states in terms of purity and fidelity evolution are less pronounced, as can be seen in Fig. 4. In this case, the scarring of map eigenstates by periodic orbits is not so strong as in the baker map case. However, scar functions are more robust than the other states, as in the previous model.

These results show that this behavior is independent of the kind of noise considered, when compared to what has been shown in [12]. There, a different open system was studied (a dissipative baker map), in which the noise was non-generic because it acts along a preferential direction in phase space, corresponding to the stable manifolds of the classical map. Also, there is no dependence on the kind of map. In fact, in a more generic system in terms of scarring like the cat map, the same has been found.

In order to propose an explanation for the behavior of

scar functions, in Figs 5 and 6 we show the Wigner distributions corresponding to the first 4 steps of the evolution of the states used in Figs. 3 and 4, respectively. In the upper panels we see the eigenstates of the maps, which have a complicated background structure along with localization on the corresponding orbit. The scar functions and POMs have a much simpler shape, with details that in general live longer than those present in the eigenstates. In fact, the eigenstates seem to converge to the corresponding scar functions. This is the underlying mechanism that produces a faster loss of fidelity and purity in the eigenstates with respect to the classically motivated quantum distributions. Finally, a brief discussion about the similar behavior of the decay of the purity and the fidelity. The first quantity measures the rate of coherence loss, that can be seen very clearly through the Wigner distributions. The second one measures the correlation between the initial state and the evolved ones. The interaction with the environment essentially destroys the interference fringes whilst the dynamics distorts the initial distributions. But all three initial states are very localized on a periodic orbit and its manifolds. Then the main initial contribution to the loss of both, purity and fidelity comes from the destruction of coherences.

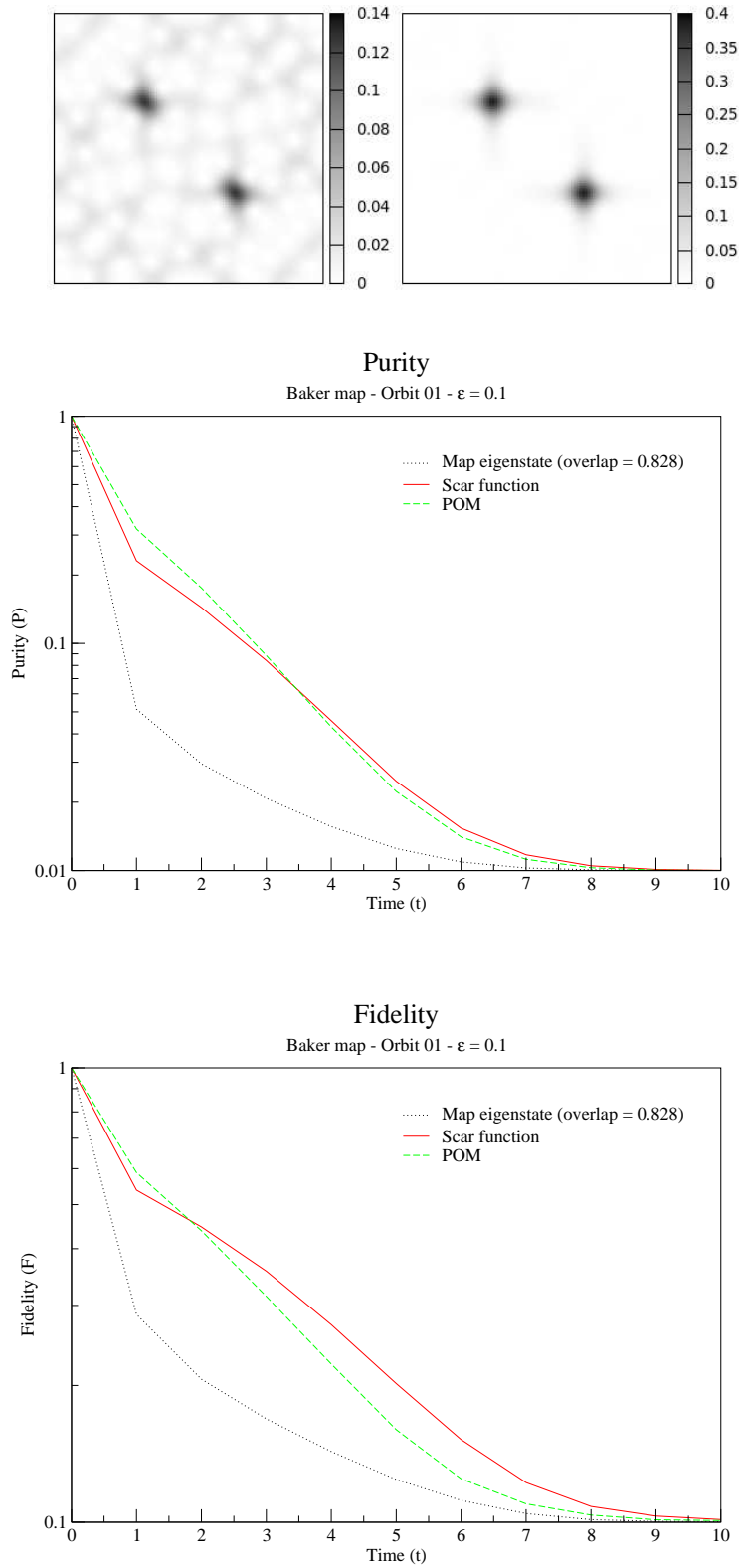


Figure 3: Purity and fidelity behavior for the noisy baker map. In the upper panels we show the Husimi representation of two initial states, localized near the period-2 orbit 01. Black corresponds to maximum probability, and white to minimum. Upper left panel: map eigenstate. Upper right panel: scar function. Middle panel: purity evolution (logarithmic scale). Lower panel: fidelity evolution (logarithmic scale). In the last two panels, black dotted lines correspond to the map eigenstate, green dashed lines to the POM, and red solid lines to the scar function. We have taken $\varepsilon = 0.1$, $N = 100$.

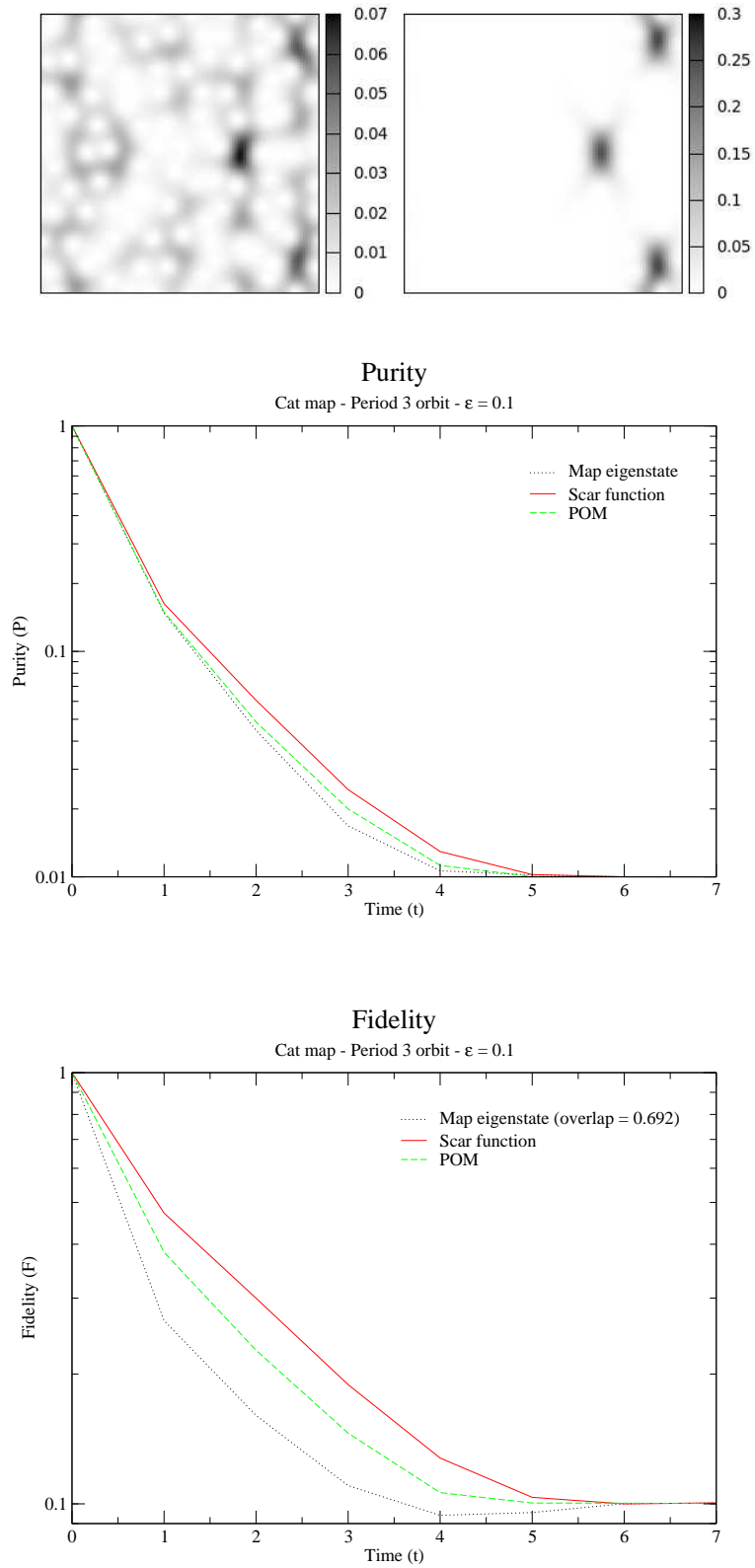


Figure 4: Purity and fidelity behavior for the noisy cat map. In the upper panels we show the Husimi representation of two initial states, localized near a period-3 orbit. Colors, patterns, scales and parameters as in Fig. 3.

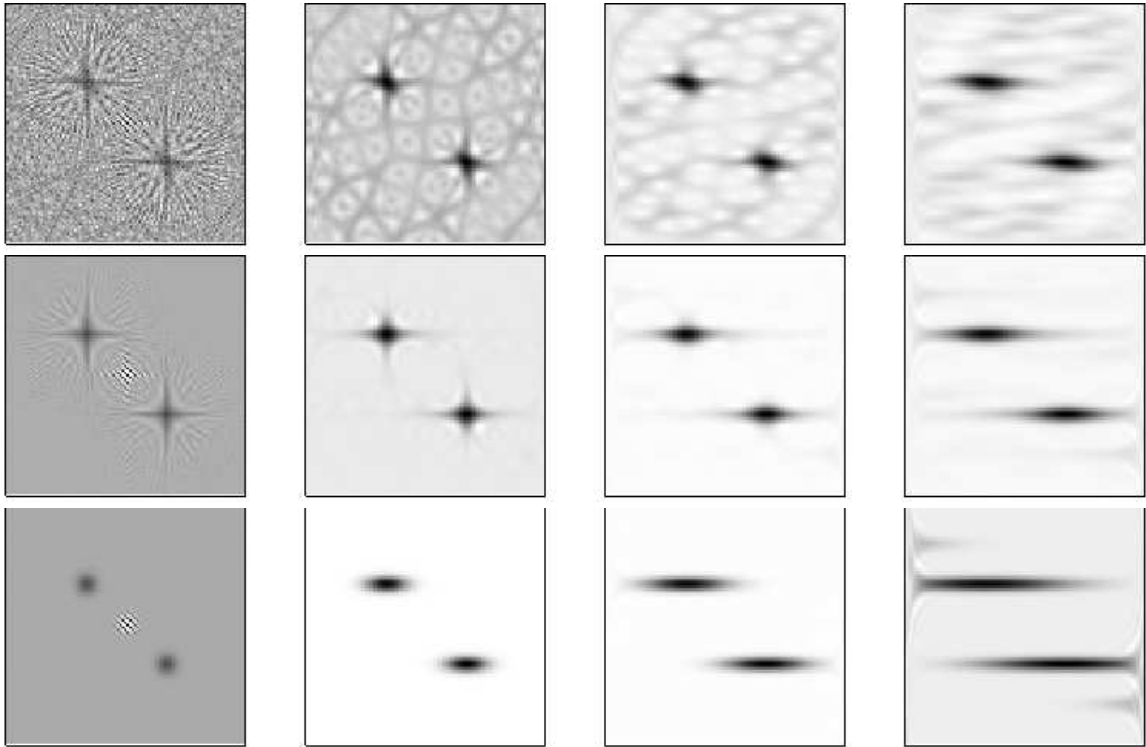


Figure 5: Wigner distributions corresponding to the first 4 steps of evolution of a baker map eigenstate (upper panels), the corresponding scar function (middle panels), and POM (lower panels). We have taken the same parameters as those chosen for Fig. 3.

V. SUMMARY AND CONCLUSIONS

We have studied two complementary decoherence measures purity and fidelity for a generic diffusive noise in two different chaotic maps.

For both quantities, we have found classical structures in quantum mechanics that are specially stable when subjected to environmental perturbations. They are the scar functions, which are associated to periodic orbits and the stable and unstable manifolds in their vicinity.

We have seen that quantum states constructed on classical invariants, periodic orbits and their stable and unstable manifolds, are more stable against an external noise than the eigenstates of the closed quantum system. This turns them into the most robust significant quantum distributions in generic dissipative maps. We conjecture that the scar functions will be the most robust structures also in general chaotic systems.

This result has already been announced for a particular dissipative noise in the Baker map. But in that case the noise was along the stable direction of the hyperbolic

structure of the original map. Here, we have confirmed the same result for a general diffusive model for two different maps.

We can then say that the external noise destroys the stability of the quantum invariants faster than the stability of the classical ones. This is a consequence of the effect of the noise as it quickly destroys quantum interferences whilst only spreads the classical structures in phase space. Despite we have only shown results for $\varepsilon = 0.1$, we have verified that they represent the generic behavior for a wide range of couplings. For strong couplings ($\varepsilon > 1$) the noise destroys the distributions very fast, and for weak ones ($\varepsilon < 0.001$) the system behaves in a similar way to the closed one.

Then, we have shown that for generic maps scar functions represent the stable classical skeleton of the map eigenstates against environmental perturbations.

We are currently developing the theory to quantitatively explain this behavior.

Acknowledgments

Support from CONICET is gratefully acknowledged.

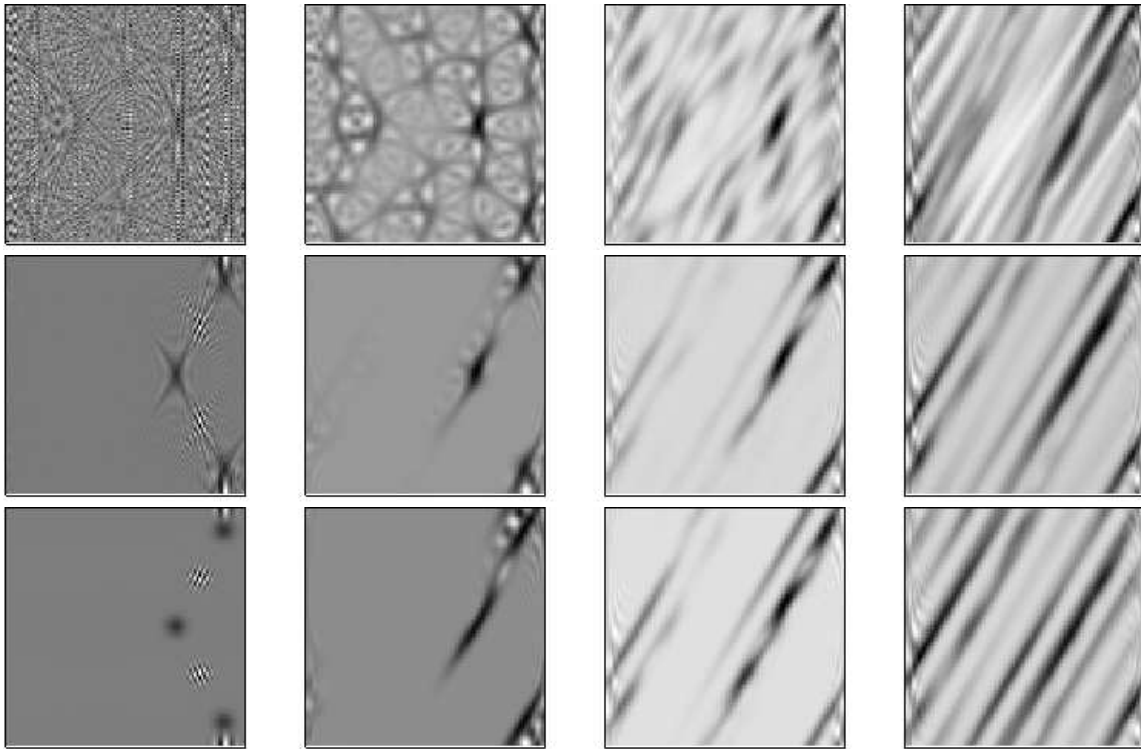


Figure 6: Wigner distributions corresponding to the first 4 steps of evolution of a cat map eigenstate (upper panels), the corresponding scar function (middle panels), and POM (lower panels). We have taken the same parameters as those chosen for Fig. 4.

-
- [1] M. Brack and R.K. Bhaduri, *Semiclassical Physics*, Addison-Wesley, Reading MA (1997).
- [2] R.N.P. Maia, F. Nicacio, R.O. Vallejos, and F. Toscano, *Phys. Rev. Lett.* **100**, 184102 (2008).
- [3] M.C. Gutzwiller, *Chaos in Classical and Quantum Mechanics*, Springer, New York (1990).
- [4] E.G. Vergini and G.G. Carlo, *J. Phys. A* **34**, 4525 (2001); A.M.F. Rivas, *J. Phys. A* **40**, 11057 (2007).
- [5] G.G. Carlo, E.G. Vergini and P. Lustemberg, *J. Phys. A* **35**, 7965 (2002)
- [6] E.G. Vergini, D.M. Schneider, A.M.F. Rivas, *J. Phys. A* **41**, 405102 (2008)
- [7] L. Ermann and M. Saraceno, *Phys. Rev. E* **78**, 036221 (2008)
- [8] W.H. Zurek, *Rev. Mod. Phys.* **75**, 715 (2003); W.H. Zurek and J.P. Paz, *Phys. Rev. Lett.* **72**, 2508 (1994); D. Monteoliva and J.P. Paz **85**, 3373 (2000)
- [9] Ph. Jacquod and C. Petitjean, *Advances in Physics* **58**, 67 (2009)
- [10] H.L. Calvo, R.A. Jalabert, and H.M. Pastawski, *Phys. Rev. Lett.* **101**, 240403 (2008)
- [11] M.V.S. Bonanca, *Phys. Rev. E* **83**, 046214 (2011)
- [12] L.A. Raviola, G.G. Carlo and A.M.F. Rivas, *Phys. Rev. E* **81**, 047201 (2010)
- [13] V.I. Arnol'd and A. Avez, *Problèmes Ergodiques de la Mécanique Classique*, Gauthier-Villars Éditeur, Paris (1967)
- [14] M. Degli Esposti and S. Graffi (eds.), *The Mathematical Aspects of Quantum Maps*, Lecture Notes in Physics 618, Springer (2003)
- [15] I. Garcia-Mata *et al.*, *Phys. Rev. Lett.* **91**, 064101 (2003); *Phys. Rev. E* **69**, 056211 (2004)
- [16] A.M. Ozorio de Almeida *Phys. Rep.* **295** 266 (1998); A.M.F. Rivas and A.M. Ozorio de Almeida, *Ann. Phys.* **276**, 223 (1999).
- [17] C. Miquel, J.P. Paz and M. Saraceno, *Phys. Rev. A* **65**, 2309 (2002).
- [18] J. Schwinger, *Proc. Nat. Acad. Sci.* **46**, 570 (1960)
- [19] M.M. Tracy, Ph.D. Thesis, University of New Mexico (2002)
- [20] C. Cohen-Tannoudji, B. Diu and F. Lalöe, *Quantum Mechanics*, vol.1, Chapter III, Hermann, Paris (1977)
- [21] M.A. Nielsen and I.L. Chuang, *Quantum Computation and Quantum Information*, Cambridge University Press (2000)
- [22] J. Preskill, *Lecture Notes for Physics 229: Quantum Information and Computation*, <http://www.theory.caltech.edu/people/preskill/ph229/>
- [23] Kraus, K., *States, Effects and Operations: Fundamental Notions of Quantum Theory*, Lecture Notes in Physics 190, Springer (1983)
- [24] P. Bianucci, J.P. Paz, and M. Saraceno, *Phys. Rev. E* **65**, 046226 (2002)
- [25] N.L. Balazs and A. Voros, *Ann. Phys.* **190**, 1 (1989)
- [26] M. Saraceno, *Ann. Phys.* **199**, 37 (1990)

- [27] J.H. Hannay and M.V. Berry. Phys. D **1**(3):267-290 (1980) VCH (2001)
- [28] W.P. Schleich, *Quantum Optics in Phase Space*, Wiley-